Available online at www.sciencedirect.com
ScienceDirect
Carbohydrate Polymers 74 (2008) 201–208
Carbohydrate Polymers
www.elsevier.com/locate/carbpol

Biocomposites of thermoplastic starch with surfactant

M. Mondragón [a,*], K. Arroyo [b], J. Romero-García [c]

[a] Instituto Politécnico Nacional, ESIME-Azcapotzalco, Sección de Estudios de Posgrado e Investigación, Av. de las Granjas 682, Col. Sta. Catarina, 02250 Mexico, D.F., Mexico
[b] Instituto Politécnico Nacional, CICATA-Altamira, km 14.5 Carr. Tampico-Puerto Industrial, 89600 Altamira, Tamps., Mexico
[c] Centro de Investigación en Química Aplicada (CIQA), Blvd. Enrique Reyna 140, 25100 Saltillo, Coah., Mexico

Received 16 January 2008; received in revised form 14 February 2008; accepted 19 February 2008
Available online 29 February 2008

Abstract

Thermoplastic starch films were prepared by a casting technique. Microfibrillated fibers from husks of corncobs were added as reinforcing agents and glyceryl monostearate (GMS) as surfactant. The films were characterized using X-ray diffraction studies, thermal and mechanical analysis and water uptake experiments. Differential scanning calorimetry (DSC) and X-ray diffraction showed the formation of amylose–GMS complexes. Compared to films without GMS the films with GMS showed significant reductions in water uptake and an increase in tensile strength. Important differences in the DSC measurements in the 160–200 °C range of films with and without GMS were also exhibited. These effects can be related to the reinforcement of the polymer matrix by the web-like network of the microfibrillated fibers, the formation of amylose–GMS complexes and the interactions of the polar groups of the GMS with the hydroxyl groups of the cellulose. Retrogradation tendencies of the TPS films were also changed by these phenomena.

Keywords: Microfibrillated fibers; Retrogradation; Starch; Surfactant; Films

1. Introduction

Development of biodegradable materials based on starch has become a very attractive option since starch can be processed as a synthetic thermoplastic polymer by the addition of plasticizers at high temperatures and high shear conditions (Hulleman, Janssen, & Feil, 1998). However, it is known that the mechanical properties of thermoplastic starch (TPS) are poor and sensitive to water content and retrogradation (Mathew & Dufrene, 2002; Van Soest, De Wit, Tournois, & Vliegenthart, 1994). Much work has been carried out to overcome these drawbacks, including blending of TPS with others polymers or using of fillers, such as natural fibers and mineral fillers (Averous & Boquillon, 2004; Carvalho, Job, Alves, Curvelo, & Gandini, 2003; Huang, Yu, & Ma, 2004; Kim, Na, & Park, 2003; McGlashan & Halley, 2003). Natural cellulose fibers are particularly attractive due to their abundance and low price as well as their renewable and low abrasive nature (Dufresne & Vignon, 1998; Hariharan & Abdul-Khalil, 2005). Cellulose fibers are composed of associated microfibrils, which can be extracted and individualized by a combined chemical and mechanical treatment (Dinand, Chanzy, Vignon, Maureaux, & Vincent, 1999). These individualized cellulose microfibrils form nanometer unit web-like networks with increased surface area, compared to natural cellulose fibers. The estimated strength of the microfibrils is at least 2 GPa (Yano & Nakahara, 2004).

It is generally accepted that long fibers provide better reinforcement to thermoplastic matrices. The short cells of the lignocellulosic materials, such as cornstalks and cornhusks, make it difficult to obtain such useful long fibers (Reddy & Yang, 2005). However due to its enlarged surface area, it could be attractive to use microfibrillated cellulose obtained from these materials for reinforcing composites. Furthermore, using microfibrillated cellulose

* Corresponding author. Tel.: +52 55 5729 6300x64514; fax: +52 55 5729 6300x46350.
E-mail address: mmondragon@ipn.mx (M. Mondragón).

0144-8617/$ - see front matter © 2008 Elsevier Ltd. All rights reserved.
doi:10.1016/j.carbpol.2008.02.004

obtained of potato, softwood, cotton and kraft the mechanical performance of composites based on thermoplastic starch has been improved (Dufresne, Dupeyre, & Vignon, 2000; Orts et al., 2004; Yano & Nakahara, 2004).

Monoacyl lipids or surfactants are used in starch-containing foods to retard retrogradation; they can interact with the amylose forming inclusion complexes (Twillman & White, 1988). These amylose lipid complexes present characteristic Vh crystalline structures with open-chain ligands forming helices having six, seven or eight D-glycosyl residues per turn. Differential scanning calorimetry (DSC) detects the amylose–lipid complexes by the presence of an endothermal transition temperature above the gelatinization value (95–135 °C) (Jovanovich & Años, 1999). It has been suggested that retrogradation is retarded by the amylose–lipid complexes given that the formation of amylose–lipid complexes is favored over the amylose retrogradation (Cui & Oates, 1999). However, to the author's knowledge no information on the amylose-lipid complexes influencing the retrogradation tendencies of TPS has been reported. Therefore, in the present study we investigated the effect of amylose–lypid complexes and microfribrillated fibers from lignocellulosic materials on physical and mechanical properties of TPS films.

2. Experimental

2.1. Materials

Dry husks of corncobs were purchased in a local store. Corn starch used in this study was obtained from MAIZENA® products. Sorbitol was purchased from Química Framce, México. All chemicals were of analytical reagent grade. Sulfuric acid, sodium hydroxide, $NaClO_2$ and Na_2SO_3 were from Fermont, México. 1-Mono-stearoyl-rac-glycerol (GMS) was from Sigma Chemical Co., USA.

2.2. Preparation of cellulose microfibrils

Cellulose microfibrils from husks of corncobs were prepared according to Dinand et al. (1999), with slight modifications. Dry husks were ground in a blade-cutting-mill to pass through a 20 mesh and, suspended in distilled water. The suspension was acidified to a pH of 2 by adding a solution of sulfuric acid and, heated to 90 °C for 2 h with constant stirring. The suspension was filtered and washed with water until the pH of the water was 7.0. The solid residue was then extracted three times with a 2% sodium hydroxide solution at 90 °C for 2 h with constant stirring. Na_2SO_3 was also added as antioxidant agent. After this treatment, it was filtered through a 0.6 mm sieve. The solid residue was washed with water until a neutral filtrate was obtained.

After a bleaching stage with a sodium chlorite ($NaClO_2$) solution in a buffer medium (caustic soda/acetic acid, pH of 4.9) at 70 ° C for 3 h, the cellulose residue was rinsed with water and freeze-dried. The purified cellulose fibers were suspended in distilled water (10 wt%) and homogenized for 10 min in a MM-1B Lourdes Vernitron homogenizer, filtered and freeze dried.

2.3. Preparation of TPS/ microfibrillated fiber films

Suspensions (5%) of starch-water were prepared. Starches were first hand-mixed with a constant amount of sorbitol 30% (dry basis of starch matrix) and then dispersed in water. Afterward, microfibrillated fibers was added at contents of 3, 5, 10 and 20 wt% (to starch + sorbitol). The fibers were previously suspended in water and dispersed by mechanical stirring for 2 h. A control film without fiber was prepared. To gelatinize starch, suspensions were first heated at boiling temperature for 1 h and then for another 1 h at 60 °C, with continuous stirring. After mixing, the suspensions were degassed under vacuum, cast in polypropylene molds and oven-dried at 60 °C for 16 h.

Another set of films were prepared using GMS adapting the method used by Cui & Oates, 1999, to prepare amylose-lipid complexes. Briefly, GMS was mixed with water at a ratio of 1:10 and heated at 60 °C for 1 h before adding to the starch-sorbitol-fiber suspensions. The dissolved GMS was added just at the beginning of the heating step at 60 °C for 1 h mentioned for the films without GMS.

2.4. Characterization of microfibrillated fibers

The microstructure of the microfibrillated fibers from husks of corncobs was evaluated by scanning electron microscopy (SEM) and transmission electron microscopy (TEM). Scanning electron microscopy (SEM) was performed to freeze dried fibers with a JEOL JSM-6100. TEM micrographs were taken with a JEOL JEM-1010 TEM, using an acceleration voltage of 60 kV. A dilute suspension of microfibrillated fibers was prepared. A drop of it was deposited on a carbon-coated grid and allowed to dry.

2.5. Characterization of films

XRD analyses were carried out on a Siemens 7KP2021 diffractometer, with CuKα radiation at 35 kV and 25 mA. The samples were scanned in step mode by 2°/min scan rate in the range $2\theta < 40$ °. All diffractograms were normalized at the same total area under the scattering curve over the measured Bragg angles.

Tensile properties were evaluated according to the ASTM D638–97 on a 4467 Instron universal testing machine at a crosshead speed of 5 mm/min. Five rectangular specimens were conditioned at 60% relative humidity (RH) for 15 days before the measurements, and the results were averaged to obtain a mean value.

Scanning electron microscopy (SEM) was performed with a JEOL JSM-6100 to the fractured surface of the tensile test specimens coated with gold/palladium on a JEOL

JFC-1100E ion sputter coater. SEM micrographs were obtained using 7 kV secondary electrons.

Thermal analysis was performed using a differential scanning calorimeter, Perkin Elmer Pyris 1 previously calibrated with indium. Samples (10 mg) conditioned at 60% RH for two weeks were put into DSC aluminum pans and sealed. The heating rate was 10 °C/min, from 50 to 200 °C.

The equilibrium water uptake was determined for all films. Circular specimens with a diameter of 3 cm were dried overnight at 100 °C. After the samples were weighed, they were conditioned at 98% RH for two weeks. The water uptake was calculated by the following equation:

$$\text{Water uptake } (\%) = \frac{M - M_0}{M_0} \times 100$$

where, M_0 represents the dried weight of the specimen and M the weight of the specimen after two weeks.

3. Results and discussion

3.1. Complex formation

The DSC was used to detect the presence of amylose–GMS complexes. Fig. 1 shows the expanded views of the derivative of the thermograms of the unfilled TPS films in the 110–140 °C range. No transitions were detected in this temperature range for the TPS film without GMS. On the contrary, an endothermic transition is confirmed for the TPS/GMS film near 131 °C which could be ascribed to the melting of crystalline amylose–GMS complexes (Cui & Oates, 1999; Le Bail et al., 1999).

3.2. Microstructure of the microfibrillated fibers

SEM and TEM micrographs of the microfibrillated fibers are shown in Fig. 2. Fibers with a ~30 μm diameter

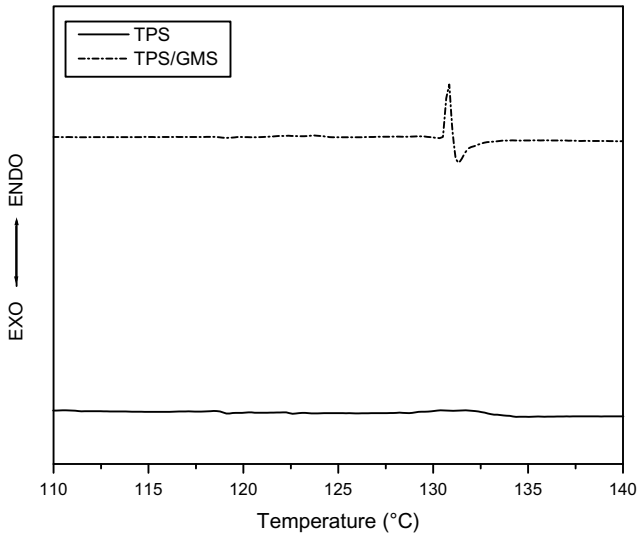

Fig. 1. Derivatives of the DSC thermograms of the unfilled fims.

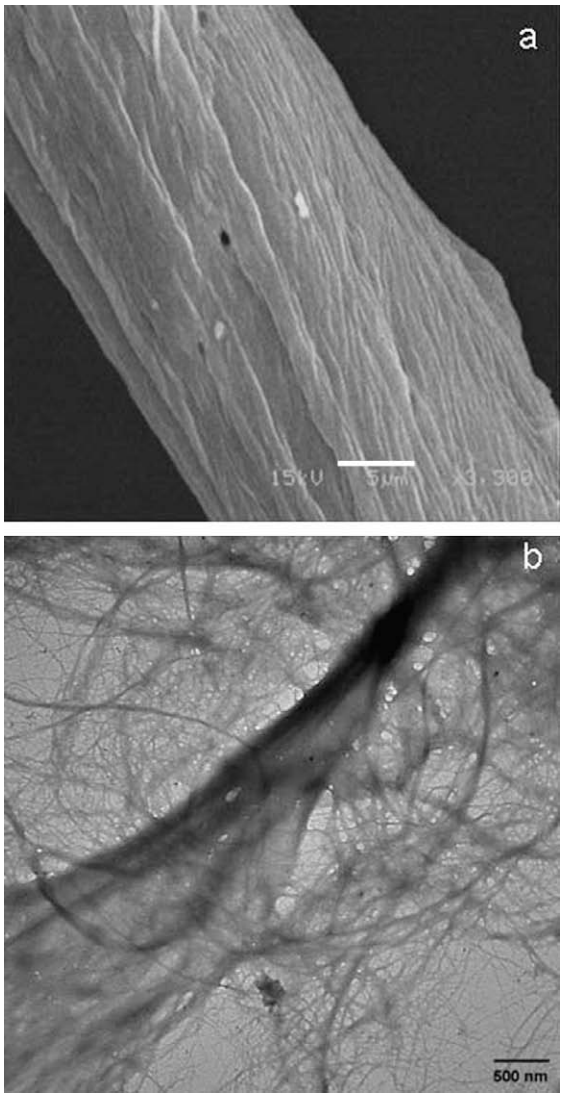

Fig. 2. SEM micrograph of cornhusks fiber (a) and, TEM micrograph of cellulose microfibrils (b).

can be seen in the SEM micrograph (Fig. 2a). However, the TEM micrograph of the dilute suspensions of these fibers shows that part of the fibers were defibrillated and form a web-like structure (Fig. 2b), as reported for other authors (Dufresne et al., 2000; Yano & Nakahara, 2004).

3.3. Morphology of the TPS/fiber films

Scanning electron microscopy (SEM) was used to characterize the morphology of the TPS/3 wt% microfibrillated fiber films. Fig. 3a and b show the tensile fractured surface of the film prepared with out GMS. The cornhusk cellulose fibers (short arrow) are quite well distributed within the TPS matrix (long arrow) due to the high compatibility between both components, which has been previously reported (Averous & Boquillon, 2004; Curvelo, Carvalho, & Agnelli, 2001). However, the fractured surface of the film prepared with GMS (Fig. 3c and d) exhibits two different

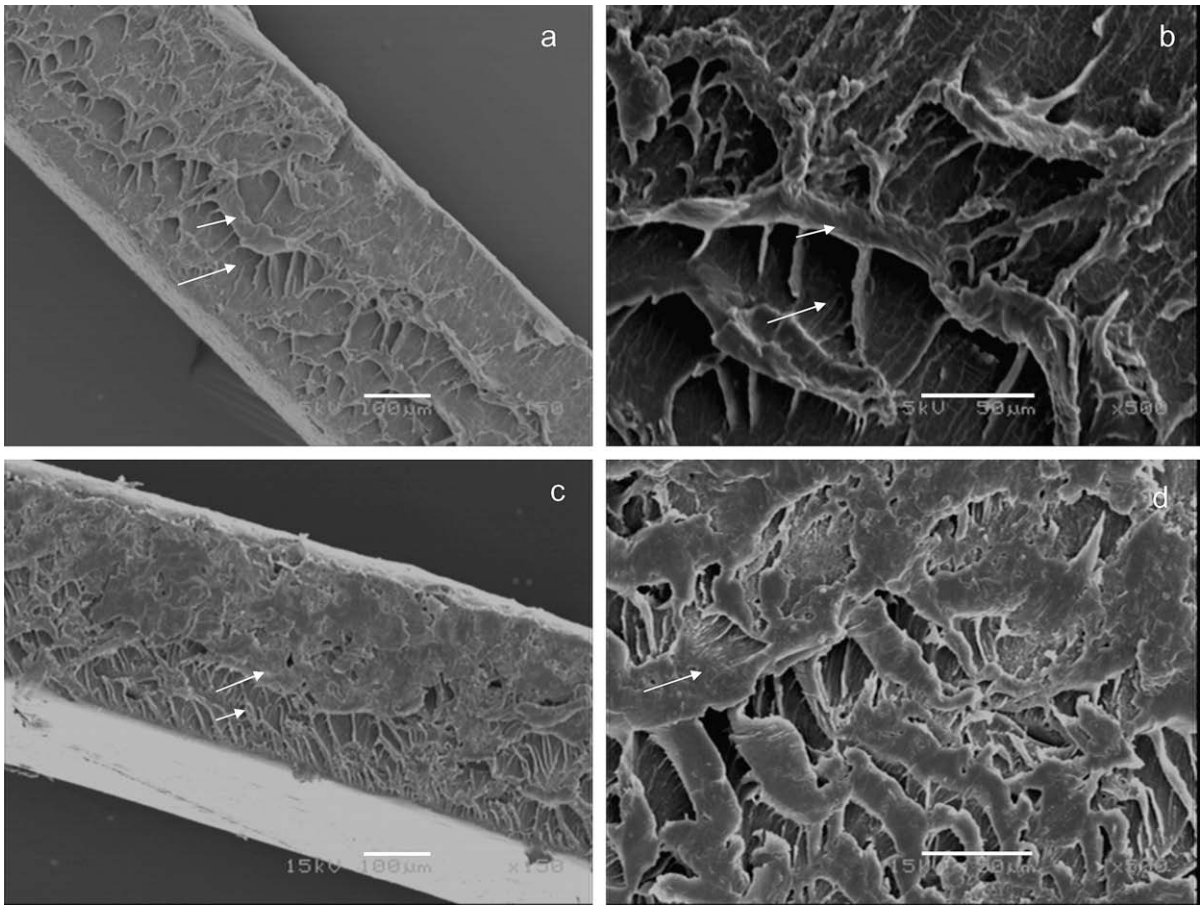

Fig. 3. SEM micrographs on the tensile fractured surface of TPS/3 wt% microfibrillated fiber films without GMS (a and b) and with GMS (c and d), at low and high magnifications.

wide zones, one zone similar to the film without GMS (short arrow) and the other one where the fibers seem to be encapsulated either individually or in groups by a layer of TPS and dispersed throughout it (long arrow). The interactions between the polar groups of the GMS molecules in the amylose–GMS complexes and the OH groups of the cellulose microfibrils could modify the interfacial adhesion between the microfibrillated fibers and the starchy matrix, promoting an encapsulated morphology.

3.4. X-ray scattering

Fig. 4 shows the X-ray diffractograms of the fiber and the TPS/fiber films at 0, 5 and 20 wt% microfibrillated fiber content. The diffractogram of the unfilled thermoplastic maize starch film, without GMS, shows major peaks at 17.1°, 20.1°, 22.3° and 26° 2θ (Fig. 4a), similar peak positions have been reported for gelatinized plasticized corn starch (Kim et al., 2003). Corn starch typically shows A-type crystalline patterns (Biliaderis, 1998). These peaks become sharper and more pronounced for the unfilled film with GMS and an additional reflection at 6.3° 2θ is shown. Theses changes can be assigned to V-type crystal structures due to amylose–GMS complexes. V-type structures show reflections at 7.4°, 13°, 17.2°, 18.6°, 20.0°, 27.8° and 31.0° 2θ (Gernat, Radosta, Anger, & Damaschun, 1993; Tharanathan & Tharanathan, 2001). The presence of amylose–GMS complexes had been previously shown by DSC (Fig. 1). The TPS films filled with 5 and 20 wt% fiber without GMS and with GMS, Fig. 4b and c, respectively, show the same crystalline structures as the TPS unfilled films, but the intensity of the peaks near of the fiber characteristic peaks (at 16° and 22.5° 2θ) increases as fiber content increases.

3.5. Mechanical properties

Figs. 5–7 show the results for the starch films with and without GMS, at several fiber contents. The Young's modulus increases from 20 to 120 MPa as fiber content increases from 0 to 20 wt%, for TPS/cellulose films prepared with or without GMS (Fig. 5). However, the modulus of the films without GMS and 3–10 wt% fiber content are lower compared to the films with GMS. The increment in stiffness of TPS films filled with cellulose has been ascribed to the formation of a hydrogen-bonded cellulose network and to the entanglement of the fibers (Anglès & Dufresne, 2000; Dufresne et al. 2000; Mathew & Dufrene, 2002). On the other hand, amylose–lipid complexes are

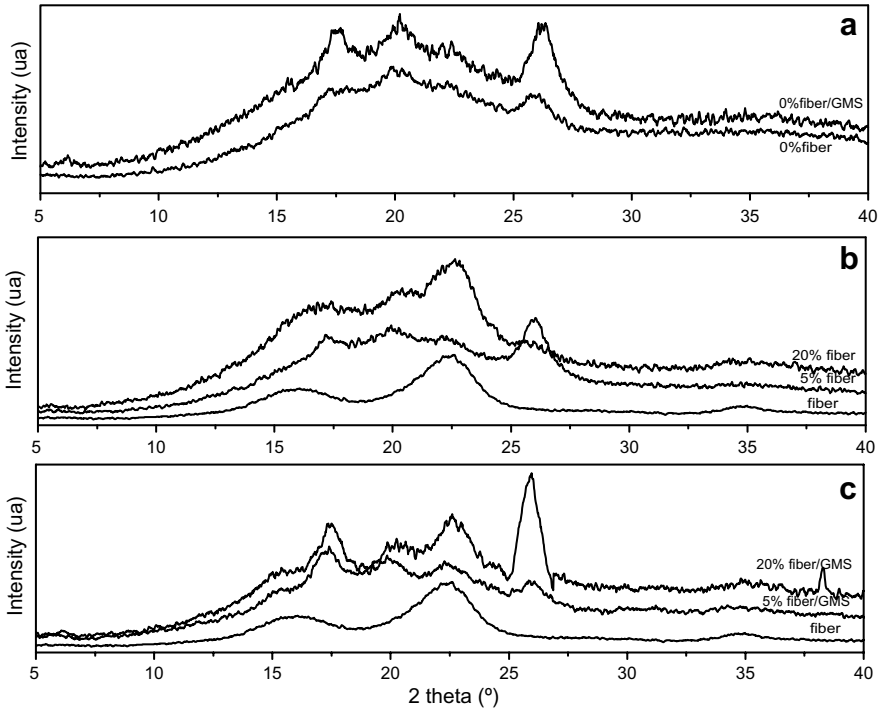

Fig. 4. X-ray diffractograms of the unfilled TPS/fiber films (a), of the fiber and the TPS/fiber films at 5 and 20 wt% microfibrillated fiber content without GMS (b) and with GMS (c).

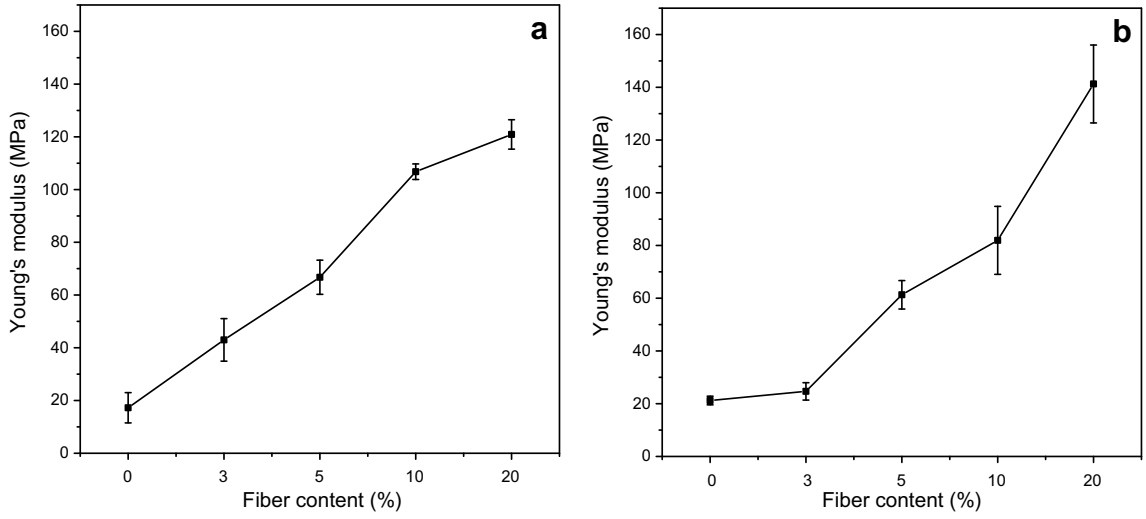

Fig. 5. Young's modulus of the TPS/fiber films without GMS (a) and with GMS (b), as a function of fiber content.

able to reduce the firmness of starchy products by helping to delay retrogradation (Cui & Oates, 1999; Krog, Olesen, Toernaes, & Joensson, 1989; Twillman & White, 1988). Therefore, the behavior of the stiffness of TPS/fiber/GMS films could be attributed a combination of both phenomena.

The tensile strength of TPS/fiber/GMS films increased significantly (from 4.5 to 14 MPa) compared to TPS/fiber films (from 2.5 to 7.7 MPa) as fiber content increases from 0 to 20 wt% (Fig. 6). Even the tensile strength of the unfilled film with GMS is higher than the unfilled film without GMS, due to the formation of complexes which cause a reduction in the mobility of the starch molecules and an increase in crystallinity (V-type crystal structures) (Cui & Oates, 1999). It is also possible that the hydrophilic ends of the GMS lying outside the helix could interact with the hydroxyl groups of the cellulose creating stronger interfaces between the TPS and the cellulose via H-bonding, in addition to the good interactions between starch and cellulose.

The elongation behavior for films with and without GMS is quite similar (Fig. 7). Both type of films has a maximum of 70% at 3 wt% fiber and afterward decreased con-

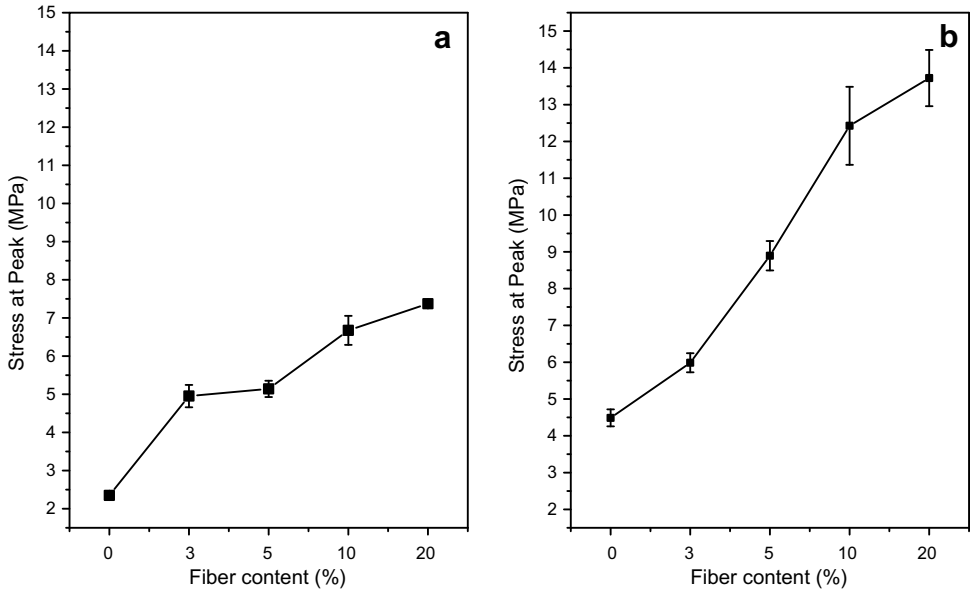

Fig. 6. Stress at peak of the TPS/fiber films without GMS (a) and with GMS (b), as a function of fiber content.

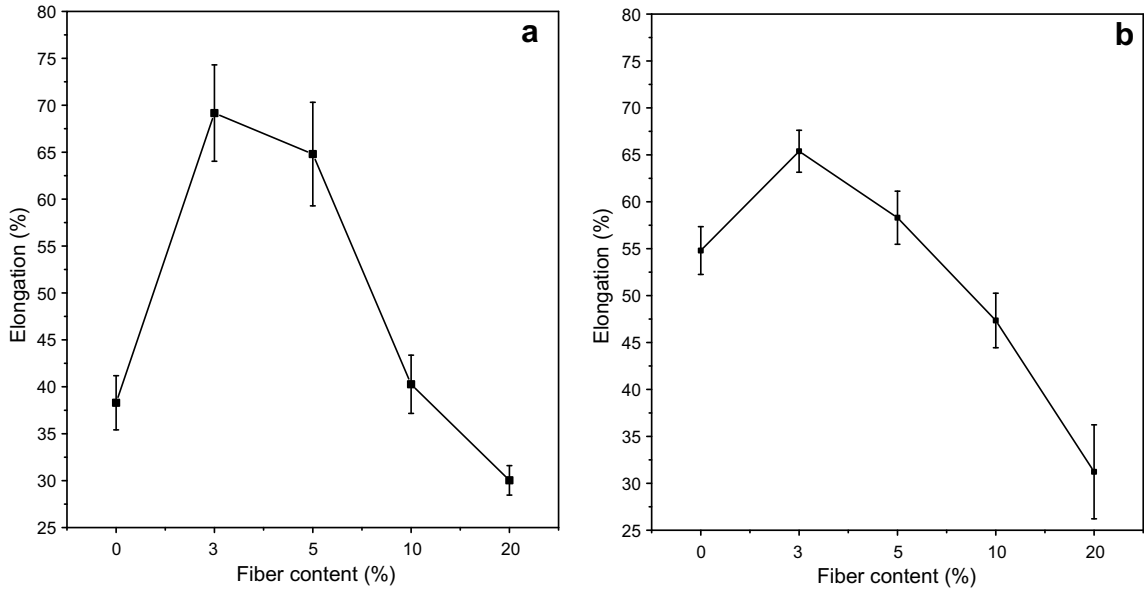

Fig. 7. Elongation of the TPS/fiber films without GMS (a) and with GMS (b), as a function of fiber content.

tinuously to 28%. The flexibility of the cellulose fibers results in higher elongation-at-break for low fiber contents however, on further addition of cellulose, the firmness of the cellulose network increases favoring the failure at low elongations. The elongation of the unfilled film with GMS was higher (55%) than the film without GMS (37%), which can be due to the increased V-type crystallinity.

3.6. Thermal analysis

Fig. 8 shows the DSC curves of the TPS/fiber films, with and without GMS. An endothermal peak is observed in the 160–200 °C range. For TPS/fiber films without GMS (Fig. 8a), the temperature position of the peak increases from 164 to 180 °C as fiber content increases from 0 to 3–5 wt%, on further addition of fiber the position of the peak decreases to 167 °C. On the other hand, for TPS/fiber/GMS films (Fig. 8b) the temperature position changes from 167 to 189, 175, 170 and 180 °C for the films containing 0, 3, 5, 10 and 20 wt% fiber, respectively. This endothermic peak has been associated with the melting of crystalline amylopectin domains reorganized during the retrogradation (Anglès & Dufresne, 2000). The changes in the position of this peak indicates that lower fiber contents favour the formation of larger crystal domains, which in

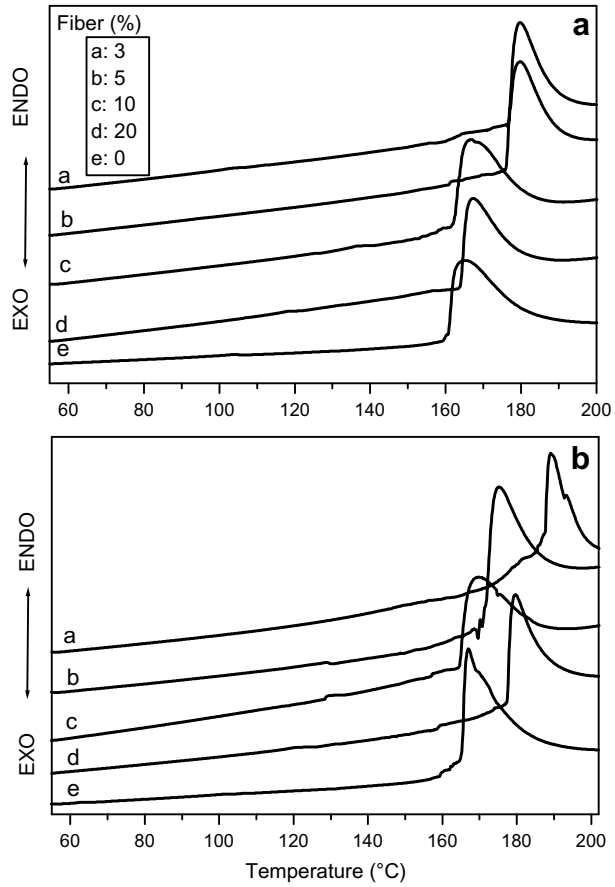

Fig. 8. DSC thermograms of the TPS/fiber films without GMS (a) and, with GMS (b).

turn lowers the mobility of the amylopectin stabilizing the retrogradation phenomenon. The higher temperature position of the peak of the TPS/fiber/GMS films also indicates a synergistic effect of the cellulose fibers and the amylose–GMS complexes to hinder the retrogradation since the crystallization of amylose–lipid complexes prevents the amylose retrogradation (Cui & Oates, 1999).

3.7. Water uptake

Fig. 9 shows the equilibrium water uptake at equilibrium for the TPS/fiber films, with and without GMS. The water uptakes of the TPS/fiber films without GMS (Fig. 9a) tend to decrease continuously from 42% to 33% as cellulose content increases from 0 to 20 wt%. While the water uptake of the TPS/fiber/GMS film (Fig. 9b), tend to decrease from 36% to 28%, but not in a continuously way. It has been reported that swelling of the TPS matrixes is reduced in presence of cellulose whiskers and microfibrils (Anglès & Dufresne, 2000). Amylose–lipid complexes also reduced the water absorption of starchy materials (Becker, Hill, & Mitchell, 2001; Galloway, Biliaderis, & Stanley, 1989) therefore; the reduced water uptake of the TPS/fiber/GMS films is due to the combined effect of the cellulose and the GMS.

4. Conclusions

Cellulose microfibrils from husks of corncobs, with web-like structures increase Young's modulus and tensile strength of TPS films due to the high interactions between the starch matrix and the increased area of the fibers. However, these mechanical properties can yet be improved by the formation of amylose–GMS complexes, which increase the V-type crystallinity and whose polar groups seem to interact with the hydroxyl groups of the cellulose. The microfibrillated fibers and amylose–GMS complexes also

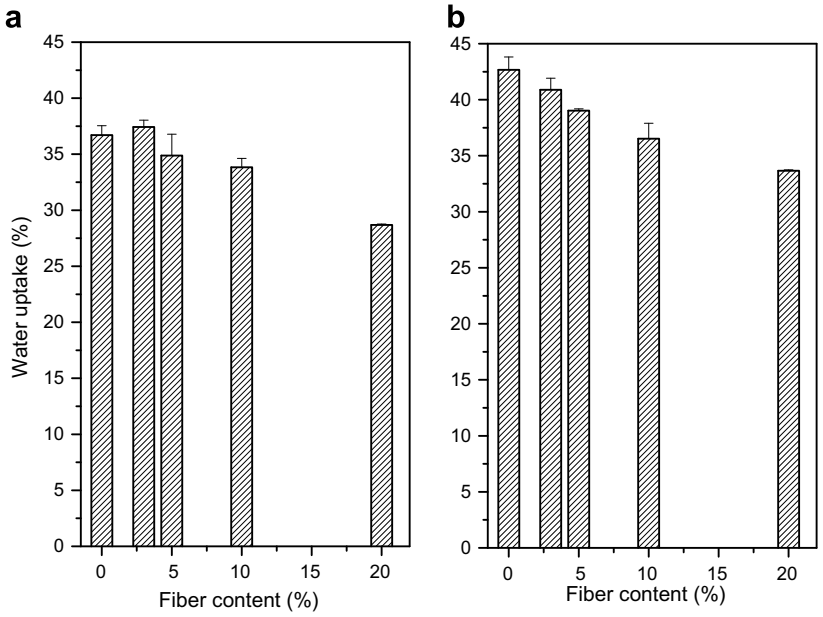

Fig. 9. Water uptake at equilibrium of the TPS/fiber films without GMS (a) and, with GMS (b).

hinder the retrogradation by lowering the mobility of the amylopectin and competing with the amylose retrogradation, respectively.

Acknowledgements

The financial support from the Secretaria de Investigación y Posgrado-IPN, is gratefully acknowledged. The authors also acknowledge M.E. Sánchez (ENCB-IPN), B.M. Huerta, C. Gonzáles and G. Padrón (CIQA) for technical assistance.

References

Anglès, M. N., & Dufresne, A. (2000). Plasticized starch/tunicin whiskers nanocomposites. 1. Structural analysis. *Macromolecules, 33*, 8344–8353.

Averous, L., & Boquillon, N. (2004). Biocomposites based on plasticized starch: Thermal and mechanical behaviors. *Carbohydrate Polymers, 56*, 111–122.

Becker, A., Hill, S. E., & Mitchell, J. R. (2001). Relevance of amylase–lipid complexes to the behavior of thermally processed starches. *Starch, 53*, 121–130.

Biliaderis, C. G. (1998). Structures and phase transitions of starch polymers. In R. H. Walter (Ed.), *Polysaccharide association structures in food* (pp. 69). New York: Marcel Dekker.

Carvalho, A. J. F., Job, A. E., Alves, N., Curvelo, A. A. S., & Gandini, A. (2003). Thermoplastic starch/natural rubber blends. *Carbohydrate Polymers, 53*, 95–99.

Cui, R., & Oates, C. G. (1999). The effect of amylase–lipid complex formation on enzyme susceptibility of sago starch. *Food Chemistry, 65*, 417–425.

Curvelo, A. A. S., Carvalho, A. J. F., & Agnelli, J. A. M. (2001). Thermoplastic starch–cellulosic fibers composites: Preliminary results. *Carbohydrate Polymers, 45*, 183–188.

Dinand, E., Chanzy, H., Vignon, M. R., Maureaux, A., & Vincent, I. (1999). Microfibrillated cellulose and method for preparing a microfibrillated cellulose. US Patent Office, Pat. No. 5,964,983.

Dufresne, A., Dupeyre, D., & Vignon, M. R. (2000). Cellulose microfibrils from potato tuber cells: Processing and characterization of starch–cellulose microfibril composites. *Journal of Applied Polymer Science, 76*, 2080–2092.

Dufresne, A., & Vignon, M. R. (1998). Improvement of starch films performances using cellulose microfibrils. *Macromolecules, 31*, 2693–2696.

Galloway, G. I., Biliaderis, C. G., & Stanley, W. (1989). Properties and structure of amylase–glycerol monostearate complexes formed in solution or on extrusion of wheat flour. *Journal of Food Science, 54*, 950–957.

Gernat, C., Radosta, S., Anger, H., & Damaschun, G. (1993). Crystalline parts of three different conformations detected in native and enzymatically degraded starches. *Starch, 45*, 309–314.

Hariharan, A. B. A., & Abdul-Khalil, H. P. S. (2005). Lignocellulose-based hybrid bilayer laminate composite: Part I-studies on tensile and impact behavior of oil palm–glass fiber-reinforced epoxy resin. *Journal of Composite Material, 39*, 663–684.

Huang, M. F., Yu, J. G., & Ma, X. F. (2004). Studies on the properties of Montmorillonite-reinforced thermoplastic starch composites. *Polymer, 45*, 7017–7023.

Hulleman, S. H. D., Janssen, F. H. P., & Feil, H. (1998). The role of water during plasticization of native starches. *Polymer, 39*, 2043–2048.

Jovanovich, G., & Años, M. C. (1999). Amylose–lipid complex dissociation. A study of the kinetic parameters. *Biopolymers, 49*, 81–89.

Kim, D. H., Na, S. K., & Park, J. S. (2003). Preparation and characterization of modified starch-based plastic film reinforced with short pulp fiber. I. Structural properties. *Journal of Applied Polymer Science, 88*, 2100–2107.

Krog, N., Olesen, S. K., Toernaes, H., & Joensson, T. (1989). Retrogradation of starch fraction in wheat bread. *Cereal Foods World, 34*, 281–285.

Le Bail, P., Bizot, H., Ollivo, M., Keller, G., Bourgaux, C., & Buleon, A. (1999). Monitoring the crystallization of amylase–lipid complexes during maize starch melting by synchrotron X-ray diffraction. *Biopolymers, 50*, 99–110.

Mathew, A. P., & Dufrene, A. (2002). Morphological investigation of nanocomposites from sorbitol plasticized starch and tunicin whiskers. *Biomacromolecules, 3*, 609–617.

McGlashan, S. A., & Halley, P. J. (2003). Preparation and characterisation of biodegradable starch-based nanocomposite materials. *Polymer International, 52*, 1767–1773.

Orts, W. J., Imam, S. H., Shey, J., Glenn, G. M., Inglesby, M. K., Guttman, M. E., & Nguyen, A. (2004). Effect of fiber source on cellulose reinforced polymer nanocomposites. In: *Proceedings of the annual technical conference 2004*. Chicago: Society of Plastics Engineers.

Reddy, N., & Yang, Y. (2005). Structure and properties of high quality natural cellulose fibers from cornstalks. *Polymer, 46*, 5494–5500.

Tharanathan, M., & Tharanathan, R. N. (2001). Resistant starch in wheat based products: Isolation and characterization. *Journal of Cereal Science, 34*, 73–84.

Twillman, T. J., & White, P. J. (1988). Influence of monoglycerides on the textural shelf life and dough rheology of corn tortilla. *Cereal Chemistry, 65*, 253–257.

Van Soest, J. J. G., De Wit, D., Tournois, H., & Vliegenthart, J. F. G. (1994). The influence of glycerol and structural changes in waxy maize starch as studied by Fourier transform infra-red spectroscopy. *Polymer, 35*, 4722–4727.

Yano, H., & Nakahara, S. (2004). Bio-composites produced from plant microfiber bundles with a nanometer unit web-like network. *Journal of Materials Science, 39*, 1635–1638.